NASA-TM-111575

Paper

ISSUES IN SPACE RADIATION PROTECTION: GALACTIC COSMIC RAYS

J. W. Wilson,* M. Kim,† W. Schimmerling,‡ F. F. Badavi,§ S. A. Thibeault,* F. A. Cucinotta,* J. L. Shinn,* and R. Kiefer†

Abstract—**When shielding from cosmic heavy ions, one is faced with limited knowledge about the physical properties and biological responses of these radiations. Herein, the current status of space shielding technology and its impact on radiation health is discussed in terms of conventional protection practice and a test biological response model. The impact of biological response on optimum materials selection for cosmic ray shielding is presented in terms of the transmission characteristics of the shield material. Although liquid hydrogen is an optimum shield material, evaluation of the effectiveness of polymeric structural materials must await improvement in our knowledge of both the biological response and the nuclear processes. Health Phys. 68(1):50–58; 1995**

Key words: radiation protection; radiation risk; risk analysis; shielding

INTRODUCTION

In the exploratory manned space missions of a few to several weeks duration of the past, only the more intense sources of space radiations, such as solar cosmic rays and trapped radiations, were considered to be the principal radiation hazards. The primary radiation protection issues were the control of early somatic effects of radiation exposure and their impact on mission safety (Billingham et al. 1965). It was reasoned that few, if any, astronauts would make more than one high profile trip to the moon so that career exposures were of secondary importance. In this context, the galactic cosmic ray (GCR) background exposures at rates of 150 to 200 mGy y^{-1} were not of great concern (Wilson 1978; Wilson et al. 1991).

With the advent of the space shuttle, the context of astronaut changed from space explorer to space worker and career exposure limits came into focus with late somatic effects seen as the ultimate limiting factor on mission activity (NCRP 1989). Such a radical shift in projected astronaut exposures led to a re-evaluation of the importance of the low level GCR background (a detailed review is given by Wilson et al. (1991)).

Within a few years of the discovery of particles of high charge and energy (HZE) as components of the GCR, the unique pattern of energy deposition on the microscopic scale raised issues with respect to effects on living cells (Schaefer 1950). Although radiobiological knowledge has greatly improved, our ability to estimate risk to the astronaut from such exposures is still quite uncertain (Schimmerling 1992). Even a crude estimate, using quality factors dependent on the linear energy transfer (LET), results in as much as 1 Sv y^{-1} exposures near solar minimum depending on shielding. There is a large potential impact on the career of a space worker, for whom low earth orbit exposure limits are currently 0.5 Sv y^{-1} (NCRP 1989) with additional total career exposure limits depending on age and sex.

Even though 1 Sv y^{-1} is a significant radiation exposure, one must hesitate before interpreting it in terms of risks to astronauts, since it implies extrapolation from the human data base for late somatic effects which are based primarily on x-ray and γ-ray exposures (BEIR V 1990). There is growing evidence of biological endpoints which are peculiar to high-LET HZE exposures that are not readily produced by x rays or γ rays. For such biological endpoints, the relative biological effectiveness (RBE) is very large or possibly undefined. Examples of these biological endpoints have been provided by the measurement of sister chromatid exchanges in resting human lymphocytes irradiated with ^{238}Pu α-particles (Aghamohammadi et al. 1988), by the observation of abnormalities in stem cell colonies surviving similar α-particle irradiation (Kadhim et al. 1992), and by the partial disintegration of chromosomes after irradiation with high-energy heavy ion beams to simulate space radiation (Kraft 1987). In these examples, the authors conclude from their experiments that, at doses comparable to that delivered by one particle (or a few particles), and for radiation effects that are not manifested for low-LET radiation (e.g., x rays), the RBE becomes infinite. Thus, new methods to predict the risk resulting from exposure to GCR radiation must be developed that are more than an extrapolation of the human

* NASA Langley Research Center Hampton, VA 23681–0001; † College of William and Mary Williamsburg, VA 23187; ‡ University Space Research Association Washington, DC 20546; § Christopher Newport University Newport News, VA 23601.

(*Manuscript received* 9 *February* 1994; *revised manuscript received* 5 *May* 1994, *accepted* 30 *July* 1994)

0017-9078/95/$3.00/0

exposure data base for low-LET exposures. Even if such a pessimistic view is unnecessary, very large RBE values have been observed for specific biological end points and the present single valued quality factor may greatly underestimate the related biological risk (Jiang et al. 1994; Thomson and Grahn 1988).

Although the complete biological response to space radiations is not understood, a guiding principle is the biological response of living tissues depends, in part, on the temporal and spatial fluctuations of the energy absorption events within the tissue system. Such fluctuations depend not only on the radiation environment to which the astronaut is exposed but how that environment is modified by interaction with the body in reaching specific tissues. Knowledge of the specific radiation types and their physical properties at the specific tissue site is required as a basis for estimating astronaut risk. Even if the environment to which the astronaut is exposed were precisely known, the energy deposition within specific tissues deep in the astronaut's body is largely known through theoretical estimates. Therefore, exposure estimates are limited by the uncertainty in the calculated models. Clearly, an accurate conversion of the astronaut's environment to estimates of exposure fields at specific tissue sites is a high priority in the solution of the space radiation protection problem.

Apart from the issues of the astronauts' self-shielding factors and the uncertainty in human response to the HZE particles, radiation shielding implies some control over the radiation environment to which the astronaut is exposed. The traditional structural material for the space vehicle has been aluminum. The absorbed dose at solar minimum from an annual GCR exposure within an aluminum shield increases from the free space value of 190 mGy to a maximum of 210 mGy behind 3–4 g cm^{-2} of shielding and declines to the free space value at about 30 g cm^{-2}. Clearly, the energy absorbed by the astronaut is not reduced by a typical spacecraft shield design and, if any protection is provided for the astronaut, it would result from changes in the microscopic inhomogeneity of the energy absorption events (Wilson et al. 1993a). These microscopic inhomogeneities depend on the physical parameters of the attenuated GCR radiation field in various materials. Herein, we develop an understanding of the qualitative changes in environmental components as a function of shield composition (including tissue equivalent shields). We investigate the role of nuclear cross sections in modifying the radiation fields and the associated effects on the microscopic distribution of the energy absorption events. Furthermore, we correlate the previously studied effects of nuclear cross section uncertainty as it applies to the uncertainty in the microscopic inhomogeneities in the energy absorption events. Using defined quality factors and a track structure dependent biological model, we interpret the modification of the radiation field by different shield materials.

MICROSCOPIC INHOMOGENEITIES

The response of living tissue to a dose D_γ of low LET radiation is represented by a sensitivity coefficient k_γ and a quadratic coefficient D_o as:

$$R_\gamma = k_\gamma D_\gamma (1 + D_\gamma / D_o) \tag{1}$$

where R_γ is either the risk of inducing a specific end point or the level of severity (e.g., prodromal syndrome). The parameter D_o is dose-rate dependent and is on the order of 1.2 Gy for late somatic effects at dose rates > 50 mGy d^{-1} (NCRP 1989, BEIR V 1990). We assume, herein, a low dose rate so that D_γ^2 may be neglected, where:

$$R_\gamma = k_\gamma D_\gamma \tag{2}$$

The energy deposits are quantized, and energy is deposited in only a fraction of cells even at career dose limits. Similarly, the energy deposited in different volumes within a given cell may also have a broad distribution. Because of this quantization of the energy absorption events, the absorbed dose D averaged over macroscopic volumes is not a good measure of biological damage. Consider the decomposition of this average quantity (Bond et al. 1988) as follows:

$$D = \frac{\sum \epsilon_i}{V N_E} = \frac{\sum \epsilon_i}{V N_H} \frac{N_H}{N_E} = \frac{\bar{\epsilon}}{V} \frac{N_H}{N_E} \tag{3}$$

where the average energy deposition event size (hit size) $\bar{\epsilon}$ is:

$$\bar{\epsilon} = \sum_i \frac{\epsilon_i}{N_H}, \tag{4}$$

and V is the sensitive site volume (unit density), ϵ_i is the energy absorbed per site hit (referred to as the hit size of the ith event), and N_E is the number of exposed sites. At low dose, not all sites are hit, so the number of site hits N_H is less than the number of sites exposed. The fraction of sites that are hit at low exposure (that is, $N_H \ll N_E$) is approximately:

$$\frac{N_H}{N_E} \approx \sigma_g \phi \tag{5}$$

where σ is the site cross section, and ϕ is the charged-particle fluence within the tissue system. The cross section can be larger than the geometric cross section of a sensitive site due to the δ-ray diffusion for which the number of site hits is increased by sites hit far from the ionizing particles path. The fluence ϕ is related to the macroscopic absorbed dose D and the unrestricted linear energy transfer (LET) L as:

$$\phi = 6.24 \frac{D}{L} \tag{6}$$

for ϕ in particles μm^{-2}, D in Gy, and L in keV μm^{-1}. For γ rays, L_γ corresponds to the average LET of the secondary electrons and has values between 0.2 and

0.5 keV μm^{-1}. The corresponding ϕ_γ is an effective secondary electron fluence that is dependent on the photoabsorption coefficient and the γ-ray fluence.

The average hit size $\bar{\epsilon}$ is one measure of the spatial inhomogeneities (also temporal fluctuations since particles arrive singly) of the energy absorption events and is known from basic physical principles and specifications of the site volume V. We have estimated $\bar{\epsilon}$ from the theory of Xapsos (1994) for various ion types as shown in Fig. 1a for a 1 Gy exposure and 0.1 μm site size corresponding approximately to the width of a single chromatin strand and its immediate environment. From eqn (3), the mean number of hits per exposed site is:

$$\frac{N_H}{N_E} = \frac{DV}{\bar{\epsilon}} \tag{7}$$

and is related to the number of hit sites shown in Fig. 1b assuming Poisson statistics. In contrast to γ rays, where many 0.1 μm sites would be hit at 1 Gy exposure, the mean hit size for energetic ions can be several keV and more, but less than 1 per thousand of the sites are, in fact, hit. The HZE particles show a smaller hit size due to δ-ray diffusion than the smaller ions at the same LET. There is a corresponding increase in the number of sites hit. A further distinction of HZE exposure is that a cluster of contiguous cells may be affected by a single ion passage due to the track core and δ-ray diffusion (Schaefer 1950), leading to correlations in the energy deposition and possible unique effects in tissue response (Todd 1983).

The microscopic inhomogeneities in number of sites hit and hit size are illustrated in Fig. 1 for various radiation field components. An added distinctive feature of the HZE exposures is that large clusters of contiguous cells are affected. The dispersion of hit size about the mean, $\sigma_\epsilon^2 = \langle(\epsilon_i - \bar{\epsilon})^2\rangle$, implies that there are fewer targets in which large hits are made and relatively more targets in which the hit size is less than the average. To the extent that any cell can be a clonogenic source of radiation-induced cancer just a few such events may suffice. Thus, HZE particles may have a RBE much greater than X rays or γ rays. Although we do not understand the radiation response to many of the GCR components, it is surely the changes wrought by shielding materials on these microscopic fluctuations which will serve as the primary means of radiation protection and not a decline in the energy absorbed with the addition of shield material.

SHIELD MATERIAL CHARACTERISTICS

Shielding the work area of an astronaut crew will always result in a wall thickness that is small in comparison with the linear dimension of the crew compartment. The shield mass is then proportional to the areal density which we use as the appropriate measure of shield thickness since two shield designs of the same areal density but different thickness result in the same shield mass. The shield properties depend on the atomic/molecular and nuclear cross sections which are still uncertain so that conclusions herein are tentative (Shinn et al. 1992; Townsend et al. 1993).

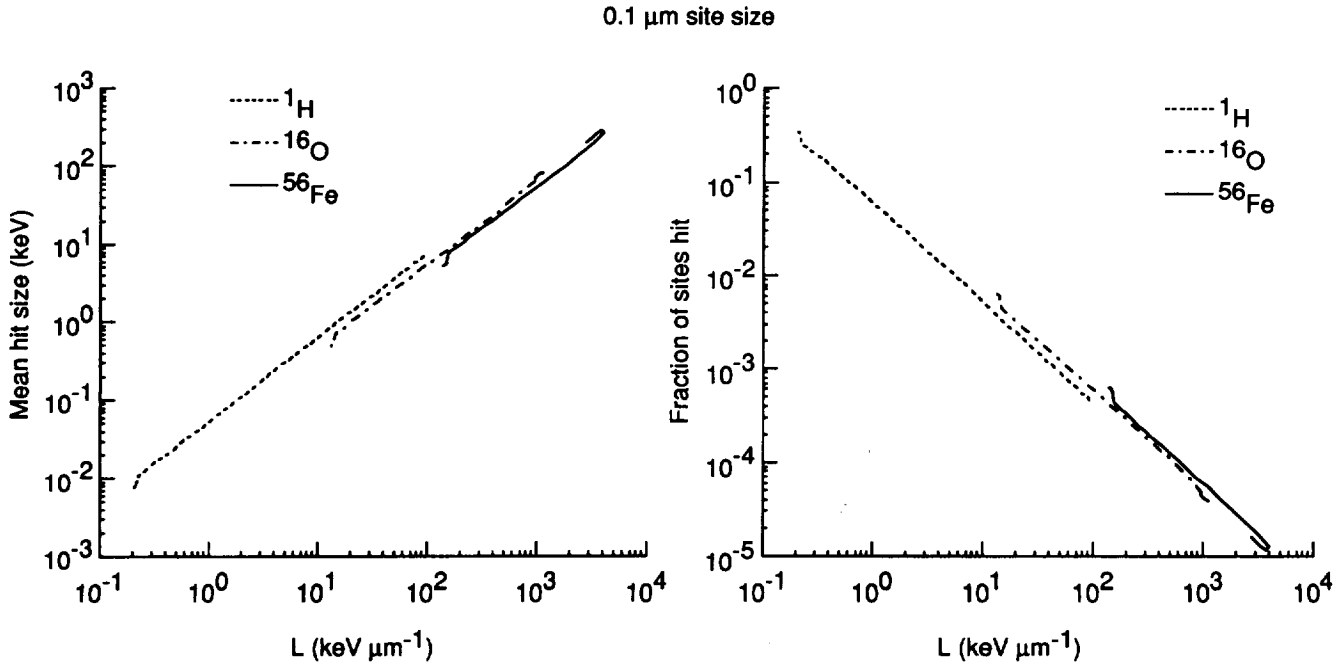

Fig. 1. Microscopic fluctuations in 0. 1 μm sites represented by: (a) mean hit size; and (b) number of sites hit.

Atomic/molecular stopping cross sections depend on the number of electrons per unit volume, the electronic mean excitation energy, and tight binding corrections for the inner shell electrons. Materials with the most electrons per unit mass, least mean excitation energy, and least tight binding corrections are most effective in stopping charged particles. Liquid hydrogen is a material at one extreme and lead is at the other extreme as an energy absorber. For example, a 825 A MeV iron ion will come to rest (loses all its energy) in 10 g cm^{-2} of liquid hydrogen but requires 38 g cm^{-2} of lead.

Nuclear cross sections relate to the mean free paths for nuclear reaction and to the nature of the reaction products. The total nuclear cross section projected by the nuclei in a unit mass of material (cm^2 g^{-1}) is the appropriate parameter and is approximately (Schimmerling et al. 1983) given by:

$$\sigma_p \simeq N_o \pi r_o^2 (A_p^{1/3} + A_T^{1/3})^2 / A_T \qquad (8)$$

where N_o is Avogadro's number, r_o is the effective nucleon radius, and $A_p(A_T)$ is the projectile (target) atomic mass number. According to eqn (8), there is a strong preference for interaction between massive projectiles and light nuclear targets. This preference for interaction with massive projectiles is greatly diminished in massive targets ($A_T >> 57$). Furthermore, there is a decline in projected nuclear cross section per unit mass as the atomic weight of the shield material increases. Equally important is the nature of the reaction products generated. Although the low Z-shields are favored by the large projected cross section per unit mass, the effects of the products generated are best seen by examining the attenuation characteristics of the GCR.

The interaction data are combined in the Boltzmann equation with the 1977 solar minimum cosmic ray spectrum (Badhwar et al. 1993) to evaluate the transmitted environment through various shields for further evaluation. The transmitted differential LET spectra ϕ_L through four shield materials evaluated using the HZETRN code (Wilson et al. 1991) are shown in Fig. 2. The left hand discontinuities (spikes which rise towards the left) are associated with the minimum ionization at relativistic energies for each ion type (Wilson and Badavi 1992). The left most discontinuity at 0.2 keV μm^{-1} is due to hydrogen isotopes followed by helium isotopes at 0.8 keV μm^{-1} and so on through *Ni* isotopes. The smaller right hand discontinuities (spikes which rise towards the right) are associated with maximum ionization in the stopping region (Bragg peak). For example, the first such peak at 100 keV μm^{-1} is due to hydrogen isotopes, and the second peak at 200 keV μm^{-1} is due to helium isotopes. It was once regarded that these stopping ions may be the primary hazard for HZE exposures (Schaefer 1950; Allkofer and Heinrich 1974). It is clear from Fig. 2 that these stopping ions are a small contribution to the total exposure. One should keep in mind that a factor of 2–3 uncertainty in the calculated LET spectrum exists for the LET region above 100 keV μm^{-1} due to uncertainty in the nuclear fragmentation cross sections (Townsend et al. 1993). Even adding energy dependence in the nuclear cross sections within HZETRN results in as much as a 50% increase above 100 keV μm^{-1} (Shinn et al. 1992).

In each case, we see the attenuation of the highest LET components in each material; liquid hydrogen is the most efficient and lead the least. Viewing the transmission curves for aluminum (Fig. 2c), one notes that the spectral changes are minimum in the several keV μm^{-1} range and that the LET spectrum attenuates at higher LET and amplifies at lower LET. This pivotal LET value is a function of the shield composition increasing to 40–50 keV μm^{-1} for lead (Fig. 2d) and dropping to less than 1 keV μm^{-1} for liquid hydrogen (Fig. 2a). The pivotal LET value is associated with the loss of a given ion species due to attenuation being matched by the production of that same species in nuclear events. The location of the pivotal LET value is critical to the changes in the microscopic inhomogeneities in the energy absorption events (expressed herein as mean hit size in a small volume and the numbers of such volumes hit) and to the biological effectiveness of the composite radiation field. For example, liquid hydrogen shows effective attenuation of all components above 1 keV μm^{-1} while lead adds to all components below about 50 keV μm^{-1} with only modest attenuation of the higher LET components. Clearly, the shield effectiveness is intimately related to the nature of the nuclear cross sections through the change in the microscopic inhomogeneities in biological exposure. Critical in this respect is the uncertainty in the nuclear cross sections. The absorption cross sections are known to 10 percent or better. The fragmentation cross sections are only known to within a factor of two.

ILLUSTRATIONS OF SHIELD EFFECTIVENESS

We examine the above concepts in terms of two biological models. The first model is the conventional risk assessment method using quality factor as a function of LET. The second model is a track structure repair kinetic model (Wilson et al. 1993b) for the mouse cell C3H10T1/2 for which there is a large body of experimental data with various ions in which repair kinetic studies were made (Yang et al. 1985, 1989). The choice of this model is dictated by the availability of data and should not be inferred to presume a known relationship to human radiation risks. We will evaluate the effectiveness of materials to reduce the biological effects for a given shield mass using these biological response models.

The distribution of absorbed dose $dD\ dL^{-1}$ at 5 g cm^{-2} depth inside an aluminum shield is shown in Fig. 3a. The absorbed dose would indicate biological response if all cells absorbed energy equally from each LET component. The quality factor is used in conven-

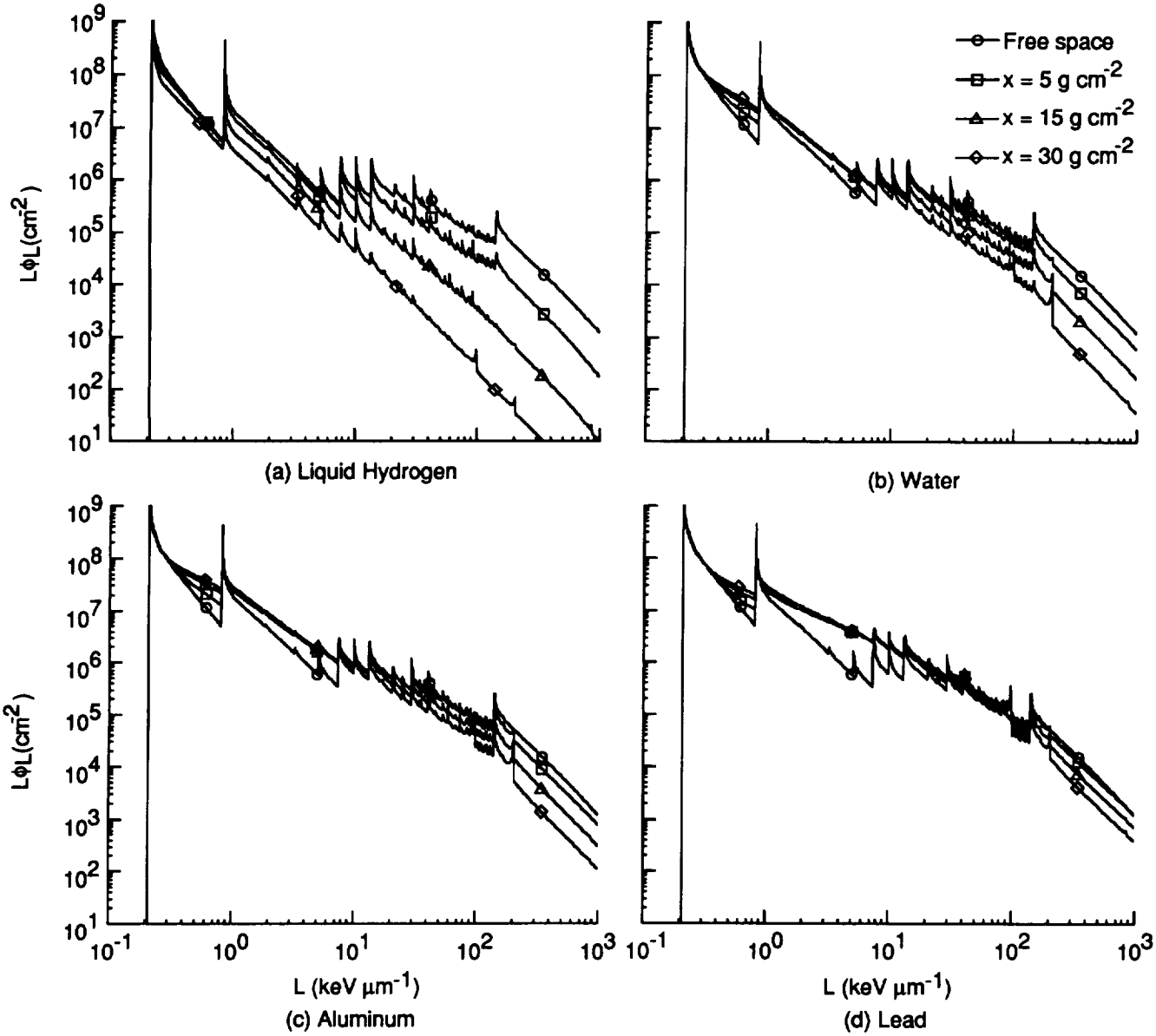

Fig. 2. Annual transmitted 1977 solar minimum GCR differential LET spectrum in four diverse shield materials.

tional dosimetry to estimate the effect that few cells are hit with large hit size by high LET components. In Fig. 3a, the dose equivalent $dH\ dL^{-1}$ distribution was obtained by multiplying the absorbed dose at each LET by the corresponding quality factor (ICRP 1991, we use the Q-L relationship on p. 81). A large contribution to dose equivalent results from ions in the LET interval from 10 to 10^3 keV μm^{-1}. These are the most significant components by conventional dosimetric standards.

The relative attenuation of dose equivalent $H(x)$ $H(0)^{-1}$ as a function of depth (in terms of areal density x) is shown in Fig. 4a. It is clear that the modification of the LET distribution as it depends on shield composition is a critical issue. Lead shielding with the LET pivot point near the peak of the LET contributions to dose equivalent is a poor shield material for the GCR environment. Clearly, the lowering of the LET pivot point enhances the material shield performance, liquid hydrogen being an optimum selection (except for structural considerations).

A second illustration is found using the model for survival and neoplastic transformation of the C3H10T1/2 mouse cells (Wilson et al. 1993b). The cellular repair model is derived from the following assumptions. Injury from γ rays follows Poisson statistics with a characteristic dose D_o and enzymatic repair is less efficient with increasing number of hits. Such a model is consistent with the concept of a high efficiency and fast but saturable repair enzyme pool in competition with a slower less efficient repair process

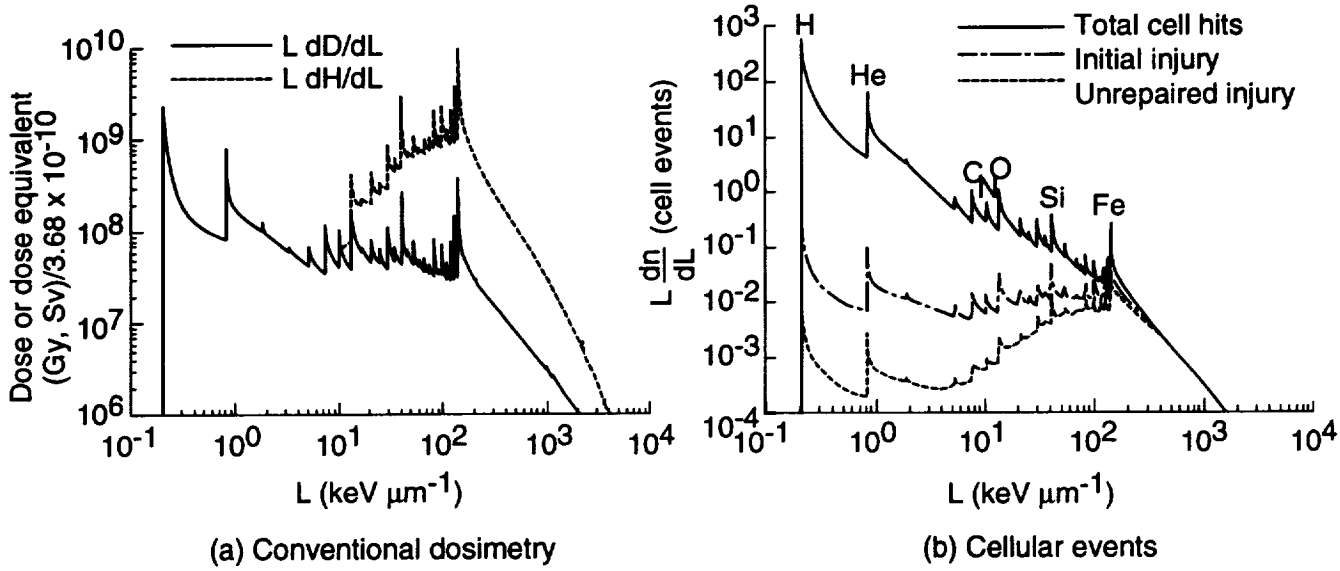

Fig. 3.(a) Differential LET-spectra for annual dose and dose equivalent with 5 g cm^{-2} aluminum shield. (b) Differential LET contributions to cell events in one year exposure behind 5 g cm^{-2} aluminum.

(Tubiana et al. 1990). Injury within a particle track is mediated by the secondary electrons (δ rays) and is related to the γ ray injury through D_o. An "inactivation" cross section associated with the core of the ion track is given (wherein the number of hits m saturate the enzyme pool) by:

$$\sigma = \int_0^* 2\pi\, t\, dt(1 - e^{-\bar{D}/D_o})^m \qquad (9)$$

where $\bar{D}$ is the average dose from the δ rays as a function of transverse distance t from the ion track (Katz et al. 1971).In the track periphery, the injury level is below saturation and multi-hit repair kinetics as in the case of γ ray exposures is assumed. It was shown by Katz that the inactivation cross section can be approximated for most ions of interest as:

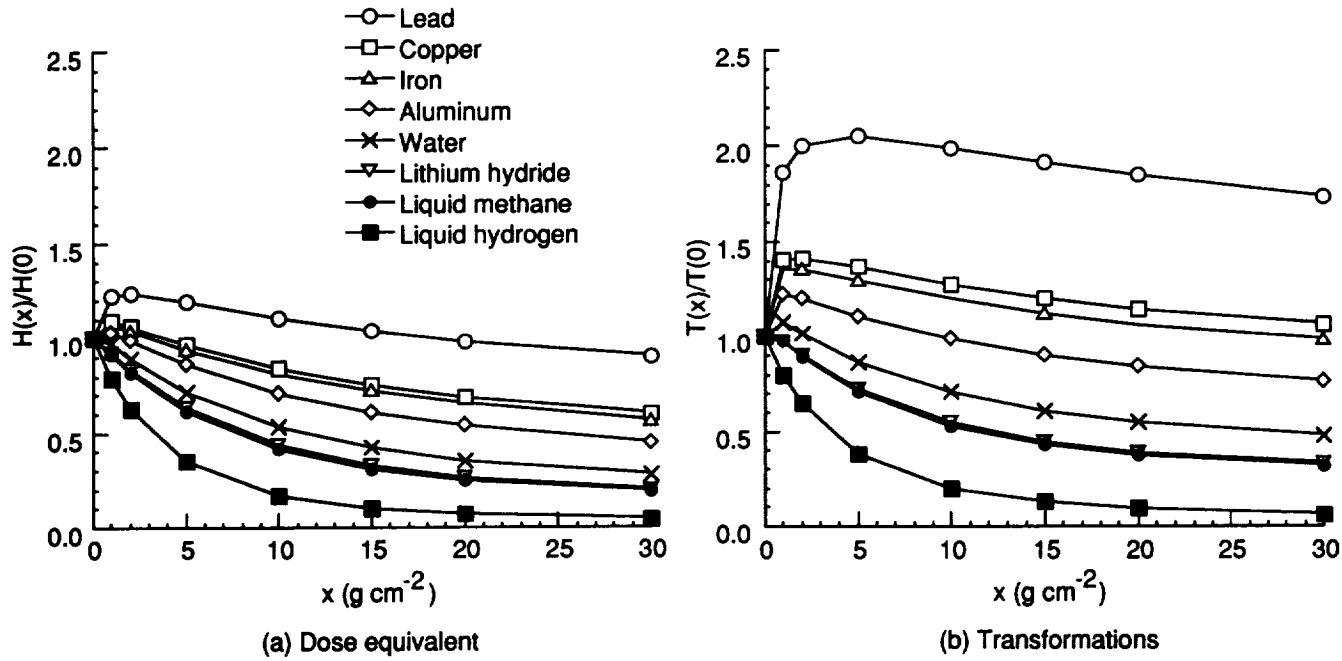

Fig. 4.(a) Attenuation of dose equivalent behind several shield materials. (b) Attenuation of cell transformation in one year exposure behind several shield materials.

$$\sigma = \sigma_0(1 - e^{-Z^{*2}/\kappa\beta^2})^m \quad (10)$$

so that the probability of direct inactivation is given as $P = \sigma/\sigma_0$ where σ_0 is the Katz "saturation" cross section. The probability of injury with multi-hit repair kinetics is $(1 - P)$. The parameter κ is a non-dimensional size parameter associated with the sensitive structure within the cell, Z^* is the ion effective charge, and β is the ion velocity in units of the velocity of light (Katz et al. 1971). In the low dose rate limit (Wilson et al. 1993b), the nonsurviving fraction of exposed cells is:

$$\frac{n_m(t)}{n_o} \approx \frac{\alpha_{m1}}{\alpha 1} 6^{1/3} \frac{(1-P)D}{D_o} + \frac{\sigma}{L} D \quad (11)$$

where D is the accumulated dose, L is the linear energy transfer, α_{m1} is the misrepair rate for once hit cells, α_1 is the total rate at which the enzyme (Z) forms a repair complex (C^*) and completes the repair through the reaction kinetics given by:

$$Z + DNA_I \rightarrow C^* \begin{matrix} \nearrow Z + DNA \\ \searrow Z + DNA_m \end{matrix} \quad (12)$$

where subscript I denotes injured DNA and subscript m denotes misrepair. Note that $(1-\alpha_{m1}\,\alpha_1^{-1})$ and $\alpha_{m1}\,\alpha_1^{-1}$ are the branching ratios of the reaction to perfect repaired and misrepaired states. A similar result holds for the fraction of transformed cells in the low dose rate limit with appropriate parameters for transformation. The repair rates and efficiencies (which depend on the cell cycle status) are found from the experiments of Yang et al. (1985, 1989) and the low dose rate limit parameters for resting G_o phase and exponential growth phase cells are given in Table 1.

Unlike conventional dosimetric analysis wherein radiation quality is represented by LET dependent factors, the repair kinetics model is driven by track-structure dependent injury coefficients. The repair kinetics model was solved at low dose rate for a $1 - y$ exposure behind the shields shown in Fig. 2. As shown in Fig. 3b, we have calculated the geometric hit frequency (taken as $\sigma_0\,DL^{-1}$ where DL^{-1} is recognized as particle fluence for fixed L), the initial level of cell injury (eqn (11) with $\alpha_{m1}\,\alpha_1^{-1} = 1$), and the unrepaired cell injury leading to clonogenic death in a C3H10T1/2 mouse cell population (Wilson et al. 1993b). Fig. 3b shows that, although the cell is most often hit by protons and helium ions, the probability of injury is small and the repair efficiency is high, with little permanent injury. Conversely, a high probability of injury and near-zero efficiency of repair occur from hits of silicon and iron ions. As a consequence, most clonogenic death from GCR exposure comes from ions with LET above 10 keV μm^{-1} (ions above relativistic carbon). Radiation injury from these ions shows minimal cellular repair. Although the two biological models are qualitatively similar in the degree of injury from various LET components, there are important track structure dependent differences.

The relative change in radiation induced transformations $T(x)\,T(0)^{-1}$ as a function of shield thickness x for a $1 - y$ exposure in space is shown in Fig. 4b. Although the attenuation characteristics for various shield materials are qualitatively similar to attenuation of dose equivalent shown in Fig. 4a, there are important quantitative differences. This is best seen in terms of the attenuation of the transformation yield in a given material compared with the attenuation of the dose equivalent in the same material. A correlation graph of the relative attenuation for transformation yield and dose equivalent is shown in Fig. 5 using the data shown in Fig. 4. If the dose equivalent represented the neoplastic transformation data then all curves would lie on a single line with unit slope.

Since the hydrogen shield reduces all LET components above a few keV μm^{-1} (LET pivotal value), the rates of attenuation of biological effects within a liquid hydrogen shield as estimated by the two risk models are similar as seen in Fig. 5. The LET pivotal

Table 1a. Cellular kinetic ratio $\alpha_{m1}\,\alpha_1^{-1}$.

	G_o phase	Exponential phase
Survival	≈0.03	0.30
Transformation	≈ .00	.01

Table 1b. Katz C3H10T1/2 cell parameters

	σ_0, cm^2	κ	m	D_0, Gy
Survival	5×10^{-7}	750	3	2.8
Transformation	7×10^{-11}	475	3	116

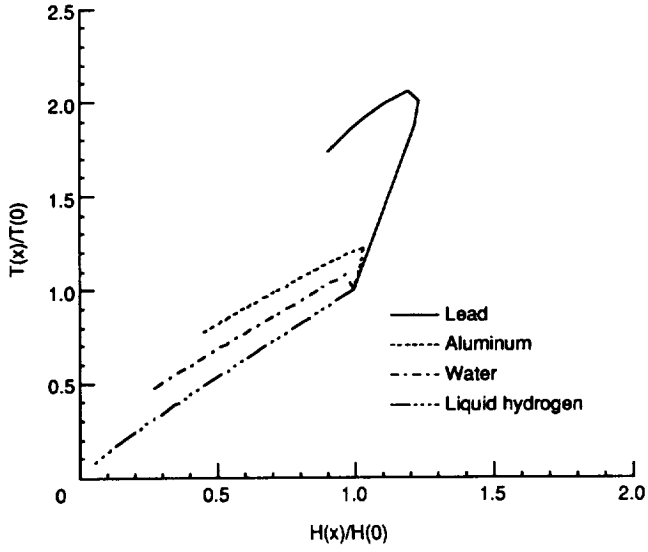

Fig. 5. Correlation of cell transformation and dose equivalent behind several shield materials. The axes indicate attenuation of effects relative to free space response.

value increases with the shield atomic number, and the mixture of ion charge and LET are radically altered for different shield materials. The two biological response models show greatly differing behavior for nonhydrogenous shields as shown in Fig. 5. Similar results are found for clonogenic death of the C3H10T1/2 cells as well (Wilson et al. 1993a). What is clear from Fig. 5 is that use of local materials (such as regolith which contains no hydrogen and consists of silicon and metal oxides) for a lunar base or martian exploration shielding designs based on quality factors may not provide the anticipated protection.

CONCLUSION

Radiation risks to astronauts depend on the microscopic inhomogeneities of energy absorption events in the specific tissues. These inhomogeneities depend not only on the space environment but the modifications of that environment by the shielding of the astronaut's surrounding structures and the attenuation characteristics of the astronaut's body. The attenuation of biological effects within the shield and body tissues depends on the biological response model and the shielding nuclear properties. Materials with low atomic number attenuate a very broad range of LET components at the expense of producing many low LET components which are less biologically damaging. Materials with high atomic number attenuate only the highest LET components at the expense of producing a broad range of LET components for which biological response may be enhanced relative to free space exposures. Clearly, the lowering of the LET pivot point is critical to the material's shield performance, liquid hydrogen being an optimum selection. Liquid hydrogen is, of course, a difficult material to use because it is a very low temperature liquid. The relative gain by use of polymer composite shield materials which are more useful in construction is a critical issue, but the final selection of the shield material must await an improved predictive methods for the biological response of astronauts to such exposure (NCRP 1989; Schimmerling 1992).

REFERENCES

Aghamohammadi, S. Z.; Goodhead, D. T.; Savage, J. R. Induction of sister chromatid exchanges (SCE) in G0 lymphocytes by plutonium-238 alpha-particles. Int. J. of Radiat. Biol. Relat. Stud. Phys., Chem. Med. 53:909–915; 1988.

Allkofer, O. C.; Heinrich, W. Measurements of cosmic ray heavy nuclei at supersonic transport altitudes and their dosimetric significance. Health Phys. 27:543–551; 1974.

Badhwar, G. D.; Cucinotta, F. A.; O'Neill, P. M. Depth-dose equivalent relationship at various solar minima. Radiat. Res. 134:9–15; 1993.

Billingham, J.; Robbins, D. E.; Modisette, J. L.; Higgins, P. W. Status report on the space radiation effects on the Apollo mission. In: Second Symposium on Protection Against Radiations in Space. Arthur Reetz, Jr., eds. Washington, DC: NASA SP-71; 1965: 39–156.

Bond, V. P.; Varma, M. N.; Sondhaus, C. A. The RBE concept, its inadequacies and a suggested replacement In: Mechanisms of radiation interaction with DNA: potential implications for radiation protection. Washington, DC: U.S. Dept. of Energy; Report No. CONF-870163; 1988; 31–38.

Committee on the Biological Effects of Ionizing Radiations. Health effects of exposure to low levels of ionizing radiation. BEIRV, Washington, DC: National Academy Press; 1990.

International Commission on Radiological Protection. 1990 recommendations of the International Commission on Radiological Protection. New York: Pergamon Press; ICRP Publ. 60; 1991.

Jiang, T. N.; Lord, B. I.; Hendry, J. H. Alpha particles are extremely damaging to developing hemopoiesis compared to gamma radiation. Radiat. Res. 137:380–384; 1994.

Kadhim, M. A.; Macdonald, D. A.; Goodhead, D. T.; Lorimore, S. A.; Marsden, S. J.; Wright, E. G. Transmission of chromosomal instability after plutonium α-particle irradiation. Nature. 355:738–740; 1992.

Katz, R.; Ackerson, B.; Homayoonfar, M.; Sharma, S. G. Inactivation of cells by heavy ion bombardmout. Radiat. Res. 47:402–425; 1971.

Kraft, G. Radiobiological effects of very heavy ions: Inactivation, induction of chromosome aberrations and strand breaks. Nucl. Sci. Appl. A3:1–28; 1987.

National Council on Radiation Protection; Measurements. Guidance on radiation received in space activities. Bethesda: NCRP; Report No. 98; 1989.

Schaefer, H. J. Evaluation of present-day knowledge of cosmic radiation at extreme altitude in terms of hazard to health. J. Aviation Med. 21:375–394; 1950.

Schimmerling, W. Radiobiological problems in space–An overview. Radiat. Environ. Biophys. 31:197–203; 1992.

Schimmerling, W.; Rapkin, M.; Wong, M.; Howard, J. The propagation of relativistic heavy ions in multielement beams lines. Med Phys. 13:212–228; 1983.

Shinn, J. L.; John, S.; Tripathi, R. K.; Wilson, J. W.; Townsend, L. W.; Norbury, J. W. Fully energy-dependent HZETRN (A Galactic Cosmic Ray Transport Code). Washington, DC: NASA; Report No. TP-3243; 1992.

Thomson, J. F.; Grahn, D. Life shortening in mice exposed to fission neutrons and x rays. VII. Effects of 60 once-weekly exposures. Radiat. Res, 115:347–360; 1988.

Todd, Paul. Unique biological aspects of radiation hazards–an overview. Adv. Space Res. 3:187–194; 1983.

Townsend, L. W.; Cucinotta, F. A.; Wilson, J. W. HZE reactions and data base development. In: Swenberg, C. E.; Horneck, G.; Stassinopoulos, E. G., eds. Biological effects and physics of solar and galactic cosmic rays. New York: Plenum Press; 1993: 787–810.

Tubiana, M.; Dutreix, J.; Wambersie, A. Introduction to radiobiology. London: Taylor and Francis; 1990: 51–57.

Wilson, J. W. Environmental geophysics and SPS shielding. In: Schimmerling, W.; Curtis, S. B. eds. Workshop on the radiation environment of the satellite power system. Berkeley: University of California; Report No. LBL-8581, UC-41; 33–116; 1978.

Wilson, J. W.; Townsend, L. W.; Schimmerling, W.; Khandelwal, G. S.; Khan, F.; Nealy, J. E.; Cucinotta, F. A.; Simonsen, L. C.; Shinn, J. L.; Norbury, J. W. Transport methods and interactions for space radiation. Washington, DC: NASA; Report No. 1257; 1991.

Wilson, J. W.; Badavi, F. F. A study of the generation of linear energy transfer spectra for space radiations. Washington DC: NASA; Report No. TM-4410; 1992.

Wilson, J. W.; Wood, J. S.; Shinn, J. L.; Cucinotta, F. A.; Nealy, J. E. A proposed performance index for galactic cosmic ray shielding. materials. Washington, DC: NASA; Report No. TM-4444; 1993a.

Wilson, J. W.; Cucinotta, F. A.; Shinn, J. L. Cell kinetics and track structure. In: Swenberg, C. E.; Horneck, G.; Stassinopoulos E. G., eds. Biological effects and physics of solar and galactic cosmic radiation. New York: Plenum Press; 1993b: 295–338.

Xapsos, M. A.; Burke, E. A.; Shapiro, P.; Summers, G. P. Energy deposition and ionization fluctuations induced by ions in small sites. Radiat. Res. 137:152–161; 1994.

Yang, T. C.; Craise, L. M.; Mei, M. T.; Tobias, C. A. Neoplastic cell transformation by heavy charged particles. Radiat. Res. 104:S-177-S-187; 1985.

Yang, T. C.; Craise, L. M.; Mei, M. T.; Tobias, C. A. Neoplastic cell transformation by high-LET radiation: molecular mechanisms. Adv. Sp. Res. 9(10):131–140; 1989.

■ ■